Quantum and semiclassical calculations of cold-atom collisions in light fields

K.-A. Suominen
Helsinki Institute of Physics, PL 9, FIN-00014 Helsingin yliopisto, Finland
and Department of Physics, Theoretical Physics Division, University of Helsinki, PL 9, FIN-00014 Helsingin yliopisto, Finland

Y. B. Band and I. Tuvi
Department of Chemistry and Department of Physics, Ben-Gurion University, Beer Sheva 84105, Israel

K. Burnett
Department of Physics, Clarendon Laboratory, University of Oxford, Parks Road, Oxford OX1 3PU, United Kingdom

P. S. Julienne
Atomic Physics Division, National Institute of Standards and Technology, Gaithersburg, Maryland 20899
(Received 7 August 1997)

We derive and apply an optical Bloch equation (OBE) model for describing collisions of ground and excited laser cooled alkali atoms in the presence of near-resonant light. Typically these collisions lead to loss of atoms from traps. We compare the results obtained with a quantum mechanical complex potential treatment, semiclassical Landau-Zener models with decay, and a quantum time-dependent Monte Carlo wave packet (MCWP) calculation. We formulate the OBE method in both adiabatic and diabatic representations. We calculate the laser intensity dependence of collision probabilities and find that the adiabatic OBE results agree quantitatively with those of the MCWP calculation, and qualitatively with the semiclassical Landau-Zener model with delayed decay, but that the complex potential method or the traditional Landau-Zener model fail in the saturation limit. [S1050-2947(98)01005-1]

PACS number(s): 32.80.Pj, 42.50.Vk, 42.50.Lc

I. INTRODUCTION

Collision dynamics of cold atoms in laser traps have been extensively investigated over the past few years. When the red detuning Δ from the atomic resonance frequency is large compared to the natural decay rate γ, we find a photoassociation spectrum of isolated bound vibrational-rotational levels in the attractive excited-state potentials. This is now a highly developed subject and is fairly well understood; see the review [1]. In contrast, when Δ is small, on the order of γ, the mechanisms and rate coefficients of trap loss processes that result from photoexcitation of the diatomic quasimolecule at long range are still rather poorly understood theoretically [2,3], in spite of the numerous experimental studies of this subject [4].

The reason for this is twofold: real hyperfine structure introduces much complexity into the collision dynamics, and the prominent role of excited-state spontaneous decay during the very long time scale of the collision is difficult to calculate quantum mechanically. The number of degrees of freedom associated with the spontaneous emission is, of course, infinite. Adiabatically eliminating these degrees of freedom leads to a mixed state representation that cannot be described in terms of wave functions but requires solving the Liouville–von Neumann equation for the quantum mechanical density matrix $\rho(R,R';t)$ [5]:

$$\frac{\partial}{\partial t}\rho(R,R';t) = -\frac{i}{\hbar}[H(R)\rho(R,R';t) - \rho(R,R';t)H(R')] + \Gamma\rho(R,R';t), \quad (1)$$

where $H(R)=T(R)+V(R)$ is the system Hamiltonian for kinetic energy $T(R)$ and interaction potential $V(R)$, and Γ is the decay tensor. Thus, the theoretical treatment of cold atom collisions serves as both prototype and paradigm for new constructs to treat nonequilibrium open systems coupled to reservoirs. Since the direct solution of Eq. (1) for cold collision situations is beyond currently available computational resources [6,7], approximate methods for treating the collision dynamics in light fields must be developed.

The methods currently available are the semiclassical local equilibrium model of Gallagher and Pritchard [8] or Julienne and Vigué [9], the semiclassical dynamical Landau-Zener models [10–13], the semiclassical optical Bloch equation (OBE) method [14], the quantum complex potential method [10,15,16], and the Monte Carlo wave packet method of simulating the full quantum density matrix [11–13]. Although the latter is capable in principle of treating the full quantum dissipative dynamics for an arbitrary number of coupled states in arbitrarily strong laser fields, the method is extremely computer intensive, and therefore slow and impractical. The complex potential method can quickly treat many coupled channels quantum mechanically, including bound state resonances, but only in the limit of very weak laser fields where no more than one excitation and decay event per collision occurs.

The semiclassical methods are very appealing because of their computational tractability, simple interpretation, and physical picture of the collision. However, several quantum calculations [11–13,16] have shown that both the local equilibrium and semiclassical OBE methods (in the formulation given in Ref. [14]) give incorrect results by an order of mag-

nitude or more for detunings of a few γ or less for temperature $T<1$ mK, depending on species. So far no practical theory exists for ultracold collisions for realistic atoms in a light field with $\Delta \simeq \gamma$, which is fully quantum mechanical and also capable of treating dissipation and decay. Therefore, there is not yet any satisfactory description of trap loss rates in the small detuning limit. For large detunings, $\Delta \gg \gamma$, collision in a light field goes to photoassociation spectroscopy, in which isolated molecular bound vibrational levels are excited. Resonant scattering theory does then an excellent job of explaining the excitation rate [1,17].

Quantum calculations have shown that semiclassical methods may still be useful in characterizing cold collisions in a light field with $\Delta \simeq \gamma$ [11–13]. The local equilibrium model for cold collisions places a prominent emphasis on off-resonant quasimolecular excitation outside the region around the Condon point R_C. In contrast to them, a semiclassical picture based on localized Landau-Zener excitation near R_C with subsequent semiclassical evolution with decay inside R_C gives an excellent representation of the quantum dynamics for T near 1 mK, when compared with results obtained from quantum mechanical calculations. The Landau-Zener model only begins to fail near $T=1$ μK and at large intensities [12]. Therefore, since there still seems to be good opportunities for semiclassical models, we have revisited the OBE method, and provided a rigorous derivation of the velocity-corrected semiclassical OBE equations starting with the appropriate quantum mechanical equations (replacing the unsatisfactory approach used in Ref. [14]). We show that an *adiabatic* rather than a *diabatic* formulation of the semiclassical OBE equations gives quite good agreement with the quantum methods, even at saturation, in contrast to the poor agreement provided by the diabatic treatment.

We find that the adiabatic OBE calculations are in good agreement with the Monte Carlo wave packet (MCWP) results and time-independent complex potential results (used for weak laser fields where this method is appropriate), down to low collision temperatures. Only upon increasing the laser detuning above the onset of resonances due to bound state structure does the adiabatic OBE method fail [10]. We also use an improved Landau-Zener model with dissipation [13], which works even in the presence of strong saturation, where the complex potential method fails. This model offers a qualitative understanding of the strong field processes. The numerical comparisons are for the standard two-state model on which the quantum and other semiclassical models have heretofore been tested. Although these test calculations ignore the complex multistate structure introduced by molecular hyperfine structure, the hope is that semiclassical methods can yet be developed that are capable of treating the complexity of multistate collision dynamics in the presence of decay.

This paper is constructed as follows. Section II presents the model of trap loss processes we shall use in order to test the methods developed and employed. Section III contains the derivation of the OBE method using the two different bases. Section IV describes the Monte Carlo method that serves as the standard against which the approximate methods we use are compared. Section V describes the complex potential method. Section VI develops the generalized Landau-Zener approach to strong laser field cold atom collisions. Section VII presents the comparison of the numerical results from the various methods, and Sec. VIII contains a summary and conclusion.

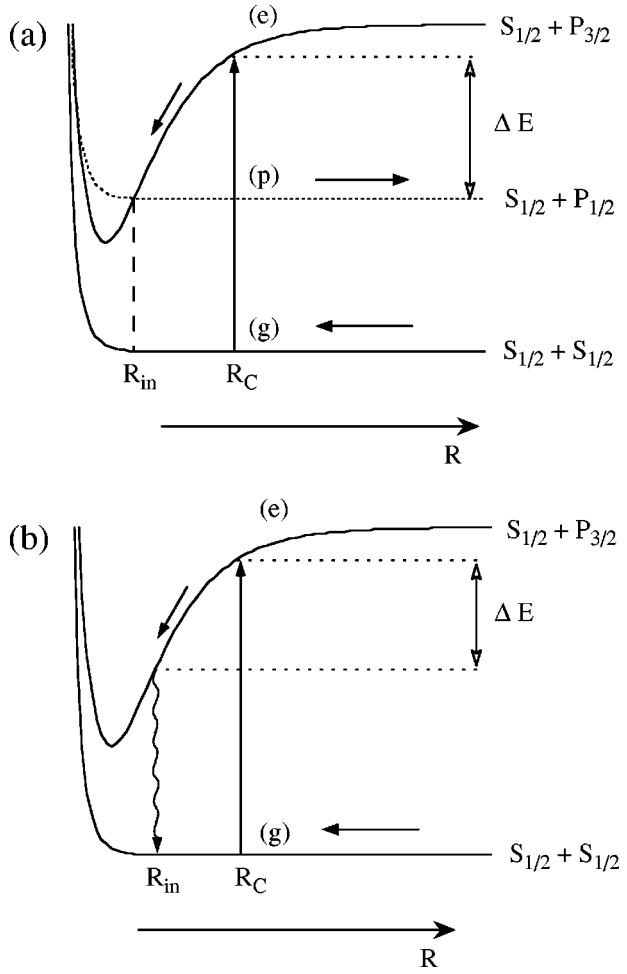

FIG. 1. The basic trap loss mechanisms. The figures show the quasimolecule potentials as functions of the internuclear separation R. The corresponding asymptotic combinations of the atomic states are also given. In (a) we demonstrate the fine-structure change (FS) loss mechanism. The quasimolecule is excited from the ground state g to the state e, then it moves towards small R, where it is transferred to the p state at $R=R_{\rm in}$. Finally the atoms exit the collision on this state, sharing a kinetic energy increase equal to ΔE. In (b) the excited state e decays back to the ground state (g) after the atoms have gained enough kinetic energy (ΔE) to escape from the trap. This is the radiative escape mechanism (RE). If decay takes place too soon, i.e., at $R>R_{\rm in}$, then the escape turns into heating due to insufficient increase in the kinetic energy (the trap depth is not exceeded).

II. THE QUASIMOLECULE MODEL FOR COLD COLLISIONS

The basic loss processes for atom traps due to cold collisions are fine-structure change (FS) and radiative escape (RE) [8,9]; these are demonstrated in Fig. 1. Due to the low temperatures we can consider the collision of two atoms as internal dynamics of a diatomic quasimolecule. The simplest prototype model for the FS mechanism consists of three collision channels, i.e., quasimolecule states. The model de-

scribed here is identical to that used in Ref. [18]. We ignore any rotational structure, i.e., only the s wave is considered, but the model can be extended to higher partial waves. Here the three channels are the ground $^2S_{1/2}+^2S_{1/2}$ state channel labeled g, the excited $^2S_{1/2}+^2P_{3/2}$ state channel labeled e, and a probe channel (correlating asymptotically with $^2S_{1/2}+^2P_{1/2}$ state) labeled p.

In the FS mechanism the system starts on channel g, and is later excited at the Condon point R_C to the channel e, which has an attractive potential. When the atom reaches the crossing between the potentials for the e and p channels, it may enter the p channel and eventually come out of the collision having gained as kinetic energy the energy difference between the $^2S_{1/2}+^2P_{3/2}$ and $^2S_{1/2}+^2P_{1/2}$ states. This gain is large enough to propel atoms from the shallow trap.

In the RE mechanism the quasimolecule decays back from the e channel to the g channel via spontaneous emission. If this decay does not take place too early, the acceleration on channel e will give the atoms enough kinetic energy to escape from the trap.

For both mechanisms we need to find out the probability for the quasimolecule to reach a certain internuclear distance $R_{\rm in}$ while still remaining on the channel e. This can be obtained from calculations by monitoring the quantum flux $J_e(R)$ on channel e directly as is done when using the OBE method, the MCWP method, and the Landau-Zener approaches (two-state case). Alternatively we can monitor the population transferred to the probe channel p, as happens in the complex potential method (three-state case).

We need a treatment that contains both the laser-induced excitation at R_C from g to e, and survival on e. Furthermore, for strong fields a proper model must allow any decayed population to be excited back to e if the decay has taken place in the vicinity of R_C. Only the MCWP method and the OBE approach can handle this reexcitation (also called population recycling) quantitatively. Further discussion on the subtle aspects of these loss mechanisms can be found, e.g., in Refs. [2–4,9].

It should be pointed out that the OBE method, the MCWP method (as we apply it in this paper), and the Landau-Zener approaches are ''one-way'' studies. We only consider the flux going in, but do not allow for any outcoming flux. For estimating the FS and RE loss this is adequate as long as the detuning of the laser is about 1–10 atomic linewidths. Then the role of bound states in the loss mechanisms is not too important yet; see Ref. [10] for more discussion. For strong fields the power broadening also diminishes the role of the bound states; most of the loss is due to processes associated with the first passage of the critical point $R_{\rm in}$ on the channel e.

We have presented elsewhere the results obtained with the adiabatic OBE method and the MCWP method in the strong field regime, and discussed the physical implications of the results [18] (the lack of saturation in trap loss when excitation becomes saturated). In this paper we study in detail the various theoretical approaches, present the general derivation of the OBE equations and their application to the two-state case (Sec. III), and show how to extend the Landau-Zener approach to the strong field regime as suggested in Ref. [13] in the case of optical shielding.

The model Hamiltonian is

$$H=T(R)\mathbf{1}+\begin{pmatrix} U_g(R)+U_c(R,l) & \hbar\Omega \\ \hbar\Omega & \hbar\Delta+U_e(R)+U_c(R,l) \end{pmatrix}, \tag{2}$$

where $T(R)$ is the radial kinetic energy operator, $U_g(R)$ is the ground electronic state which behaves asymptotically as $U_g(R)=C_6/R^6$, $U_c(R,l)=\hbar^2 l(l+1)/2\mu R^2$ is the centrifugal potential, μ is the reduced mass of the quasimolecule (we assume a Cs_2 system), $U_e(R)$ is the excited-state potential correlating asymptotically to $^2S_{1/2}+^2P_{3/2}$ alkali atoms and behaving asymptotically as $-C_3/R^3$, and Δ is the detuning from resonance, $\hbar\Delta=E(P_{3/2})-E(S_{1/2})-\hbar\omega$. Here ω is the laser frequency, and the laser-induced coupling is described by the Rabi frequency Ω. The g and e channel potentials cross at the Condon point $R_C(\Delta)$ where $\hbar\Delta=U_e(R_C)-U_g(R_C)$. This crossing occurs at large internuclear distances. The values used for potential parameters are $C_3=20.30\ e^2a_0^2$ and $C_6=6.40\times10^5 e^2a_0^2$, where e is the electron charge and $a_0=0.529$ Å is the Bohr radius [9,18]. Note that we express all energy and angular frequency parameters in frequency units.

In studies using different laser parameters we have selected for a suitable inner distance $R_{\rm in}=143a_0$, although the methods that we use allow the determination of $J_e(R)$ for all values of R. The atomic excited state has a linewidth $\gamma_{\rm at}=5.13$ MHz, and we have taken the molecular linewidth to be $\gamma=(4/3)\gamma_{\rm at}$, independent of R. And as mentioned above, we consider only the case $l=0$.

A reasonably complete description of cold atom collision dynamics in laser traps can be obtained via the time-dependent density matrix $\rho(R,R';t)$ satisfying the Liouville equation (1). The probability of reaching the inner region on the excited-state potential (or the particle flux in the inner region on the excited state potential) can be determined directly from the diagonal density matrix elements $\rho_{ii}(R_{\rm in},R_{\rm in};t)$. However, the direct numerical solution for the density matrix is presently beyond our capabilities for the cold atom collision problem. Instead we shall use various approximations to solve for the dynamics. The time-dependent MCWP approach basically includes all the physics contained in the Liouville equation, and it will provide the standard against which all other methods are to be judged.

Our model is a simplified representation of the true collision situation. Experiments have shown that inclusion of hyperfine structure is necessary to properly treat the collisions of laser cooled alkali species [4,19]. It is exactly for this reason that it is so important to develop simple and accurate approximate numerical methods that can conceivably be used on problems including hyperfine dynamics where a large number of channels is required to treat the manifold of the hyperfine states.

III. OPTICAL BLOCH EQUATIONS

A. General situation

In this section we derive the semiclassical optical Bloch equations. We start with the Liouville equation (1) and use Wigner function description into which we introduce semiclassical approximations. If we write Eq. (1) by components we get

$$i\hbar\frac{\partial}{\partial t}\rho_{ij}(R,R';t)=-\frac{\hbar^2}{2\mu}\left(\frac{\partial^2}{\partial R^2}-\frac{\partial^2}{\partial R'^2}\right)\rho_{ij}(R,R';t)$$
$$+\sum_k\left[V_{ik}(R)\rho_{kj}(R,R';t)\right.$$
$$\left.-\rho_{ik}(R,R';t)V_{kj}(R')\right]$$
$$+i\hbar\sum_{kl}\Gamma_{ijkl}\rho_{kl}(R,R';t). \tag{3}$$

Here we have explicitly written out the kinetic and potential energy parts of the Hamiltonian H; the term $V(R)$ contains the potentials for the internal states of the quasimolecule and couplings between them. We assume that V has no time dependence as we have eliminated the oscillating laser field terms using the rotating-wave approximation and an appropriate phase shift (here V contains the potentials U and couplings $\hbar\Omega$).

It should be pointed out that our description is time dependent, so instead of the boundary conditions used in the time-independent scattering theory we have an initial value problem, i.e., we solve Eq. (3) starting at $t=t_0$ with some initial density matrix $\rho(R,R';t_0)$. If Eq. (3) corresponds to a closed system (no decay out of the selected set of levels), then ρ can have steady-state solutions.

Typically one takes as the initial state the steady state result corresponding to atoms being well separated, with the quasimolecule potentials being flat over the distance that the system moves within the time it takes to establish the steady state. In other words, the molecular potentials do not impose any dynamics that would interfere with the steady state formation.

In time-independent scattering theory the initial conditions cannot be stated in terms of diabatic states if couplings between the states do not disappear asymptotically, as is the case with laser-induced quasimolecule processes. However, since the system at large R evolves quickly into the local steady state, which is independent of the selected basis states, there is no *a priori* reason to regard the adiabatic basis better than the diabatic basis. In practice one tends to choose the diabatic basis, because it allows a simple description of the spontaneous emission processes. Furthermore, as discussed below, we can select *any* initial state in *any* basis, if we allow the system initially enough time to reach locally at large R a steady state before the spatial dependence of the quasimolecule potentials will couple the steady state formation and molecular dynamics. In the following derivation of the optical Bloch equations we shall first use the diabatic basis, and then transform it into the adiabatic basis case.

We assume for simplicity that in our current description Γ is independent of position, but it is easy to extend our treatment to allow R dependence in Γ; such dependence can easily arise if retardation effects are properly included to the quasimolecule potentials and lifetimes. We redefine our spatial coordinate system by writing $R=r+q/2$, $R'=r-q/2$, which transforms the kinetic term:

$$\frac{\partial^2}{\partial R^2}-\frac{\partial^2}{\partial R'^2}=2\frac{\partial}{\partial r}\frac{\partial}{\partial q}. \tag{4}$$

The density matrix $\rho(R,R';t)$ contains information about the spatial coherences in the system. In order to calculate quantum fluxes at some interatomic distance R we do not need all that information, but only the spatially diagonal elements $\rho(R,R;t)$. However, the evolution of these diagonal elements depends on the off-diagonal $\rho(R,R';t)$ elements. By using the Wigner function [20]

$$W_{ij}(p,r;t)=\int_{-\infty}^{\infty}dq\exp(-ipq/\hbar)\rho_{ij}(r+\tfrac{1}{2}q,r-\tfrac{1}{2}q;t) \tag{5}$$

we can include the spatial coherences and yet effectively work with the spatially diagonal terms only.

First we apply the Fourier transform given in Eq. (5) on both sides of Eq. (3) in order to obtain the equation of motion for the Wigner function:

$$\frac{\partial}{\partial t}W_{ij}(p,r;t)+\frac{p}{\mu}\frac{\partial}{\partial r}W_{ij}(p,r;t)=\int_{-\infty}^{\infty}dq\exp(-ipq/\hbar)\left\{\frac{1}{i\hbar}\sum_k\left[V_{ik}(r+q/2)\rho_{kj}(r+q/2,r-q/2;t)\right.\right.$$
$$\left.\left.-\rho_{ik}(r+q/2,r-q/2;t)V_{kj}(r-q/2)\right]+\sum_{kl}\Gamma_{ijkl}\rho_{kl}(r+q/2,r-q/2;t)\right\}. \tag{6}$$

One should note that above we have applied integration by parts in order to replace $-i\hbar(\partial/\partial q)$ with p; this requires that $\lim_{q\to\pm\infty}\rho(r+\frac{1}{2}q,r-\frac{1}{2}q;t)=0$, i.e., that the spatial coherences disappear as we move away from the diagonal—this is a reasonable assumption.

If we integrate the Wigner function over momentum p we get the spatial probability distribution, which we can define as

$$\tilde{\rho}_{ij}(r,t)=\frac{1}{2\pi\hbar}\int_{-\infty}^{\infty}dp\,W_{ij}(p,r;t). \tag{7}$$

The quantity $\tilde{\rho}_{ij}(r,t)$ equals $\rho_{ij}(r,r;t)$, as can readily be seen by substituting the expression for $W_{ij}(p,r;t)$ in Eq. (5) into the right hand side of Eq. (7) and carrying out the integration over p. So, by integrating Eq. (6) over p we get the equation of motion for $\tilde{\rho}_{ij}(r,t)$:

$$\frac{\partial}{\partial t}\tilde{\rho}_{ij}(r,t)+\frac{1}{\mu}\frac{\partial}{\partial r}\left[\frac{1}{2\pi\hbar}\int_{-\infty}^{\infty}dpp\,W_{ij}(p,r;t)\right]=\frac{1}{i\hbar}\sum_{k}\left[V_{ik}(r)\tilde{\rho}_{kj}(r;t)-\tilde{\rho}_{ik}(r;t)V_{kj}(r)\right]+\sum_{kl}\Gamma_{ijkl}\tilde{\rho}_{kl}(r,t). \tag{8}$$

Here we have used the fact that there is no p dependence on the right-hand side of Eq. (6), so that if we perform the momentum integration first, we obtain a $\delta(q)$ function, and thus the integration over q merely sets $q=0$.

If a convenient method of evaluating the kinetic term were available, we could use the result (8) to obtain exactly the diagonal elements of $\tilde{\rho}$ at given r and t, $\tilde{\rho}_{ii}(r,t)$, which is the probability of being in channel i at position r and time t. However, since we do not have any exact methods for calculating the second term in Eq. (8), we shall estimate it using a WKB approach. The WKB approximation for the density matrix element is given by

$$\rho_{ij}(R,R';t)\simeq\frac{a_i(R;t)a_j^*(R';t)}{\sqrt{p_i(R)p_j(R')}}\exp\{i[\beta_i(R)-\beta_j(R')]/\hbar\}, \tag{9}$$

where $p_i(R)$ is the local classical momentum in state i, $\beta_i(R)$ is the action at R,

$$\beta_i(R)=\int^{R}dx\;p_i(x), \tag{10}$$

and $a_i(R,t)$ is the amplitude factor for the WKB wave. We consider only the incoming wave, which fixes the sign of the β terms, and assume that a_i and p_i do not depend on position very strongly. Furthermore, we assume that the classical momenta $p_i(R)$ are nonzero and real. It should be noted that by introducing the classical momenta we have made our equations energy dependent as well, since

$$p_i(r)=\sqrt{2\mu\{E-[V_{ii}(r)-V_{ii}(\infty)]\}}, \tag{11}$$

where E is the asymptotic energy for the WKB wave (equal to the asymptotic relative kinetic energy of the colliding atoms).

It should be noted that our definition (11) of the classical momenta is clearly different from the one encountered in the traditional scattering theory, if we consider the asymptotic situation. In the time-independent theory the channels (states) are typically either open or closed, depending on the collision energy, i.e., their classical (WKB) momenta are asymptotically either real or imaginary. This is because they are defined as $p_i^{\rm scatt}(r)=\sqrt{2\mu\{E-[V_{ii}(r)-V_{00}(\infty)]\}}$, where $i=0$ corresponds to the channel of the ingoing wave, defined by the asymptotic boundary conditions.

The difference here is due to the presence of the relaxation terms in Eq. (3), and is required by the asymptotic situation. In the time-dependent treatment we have $p_i(\infty)=\sqrt{2\mu E}$, which is independent of the state label i. This is because asymptotically we have a steady state formation that is not coupled to the dynamics because the potentials are flat. For simplicity we base our following discussion on a two-state system. Assuming that the excited-state and ground-state populations had different asymptotic momenta, the steady-state formation (the cycles of excitation and decay) quickly mixes these populations and eventually the distribution of momentum on the ground state and the excited state would be exactly equal. In other words, because of decay we can have asymptotic population even on a closed channel, but this population is a steady-state reflection of the ground-state population and must have the same classical momentum. This result is independent of the selected basis. However, as we fix the asymptotic situation by using Eq. (11), we introduce other problems, which will be discussed in Sec. III C.

Next we insert Eq. (9) into Eq. (5), and use the result in Eq. (8). The exponential part of the integrand can be expanded around r:

$$\begin{aligned}\exp\{i[\beta_i(r+\tfrac{1}{2}q)-\beta_j(r-\tfrac{1}{2}q)]/\hbar\}&\\ \simeq\exp\{i[\beta_i(r)-\beta_j(r)]/\hbar+i\tfrac{1}{2}[p_i(r)+p_j(r)]q/\hbar&\\ +\mathcal{O}(r^2)\}.&\end{aligned} \tag{12}$$

Then we apply the stationary phase method to obtain

$$\frac{1}{2\pi}\int_{-\infty}^{\infty}dpp\,W_{ij}(p,r;t)=\tfrac{1}{2}[p_i(r)+p_j(r)]\tilde{\rho}_{ij}(r,t). \tag{13}$$

Substitution of this expression into Eq. (8) yields

$$\begin{aligned}\frac{\partial}{\partial t}\tilde{\rho}_{ij}(r,t)+\frac{1}{2\mu}[p_i(r)+p_j(r)]\frac{\partial}{\partial r}\tilde{\rho}_{ij}(r,t)&\\ =\frac{1}{i\hbar}\sum_{k}\left[V_{ik}(r)\tilde{\rho}_{kj}(r;t)-\tilde{\rho}_{ik}(r;t)V_{kj}(r)\right]&\\ +\sum_{kl}\Gamma_{ijkl}\tilde{\rho}_{kl}(r,t).&\end{aligned} \tag{14}$$

Here we have assumed that the classical momenta vary so little with r that they can be taken outside the derivative term.

Our aim is to find the total incoming quantum flux at each position r (integrated over all times), and thus we are not interested in the actual time dependence. This simplifies our model to a great extent. Now the total flux can be obtained as a steady-state result from Eq. (14). Since our model corresponds to a ''one-way'' situation, the steady-state flux at r is equal to the total flux that has passed that point. In the steady state the time derivative in Eq. (14) vanishes, and we can replace $\tilde{\rho}_{ij}(r,t)$ by $\langle\tilde{\rho}_{kl}\rangle_{\rm ss}(r)$. Furthermore, it is convenient to define the quantity

$$\sigma_{kl}(r)\equiv\sqrt{p_k(r)p_l(r)}\langle\tilde{\rho}_{kl}\rangle_{\rm ss}(r) \tag{15}$$

whose diagonal elements give the flux in the various states at position r. We shall call this quantity the semiclassical den-

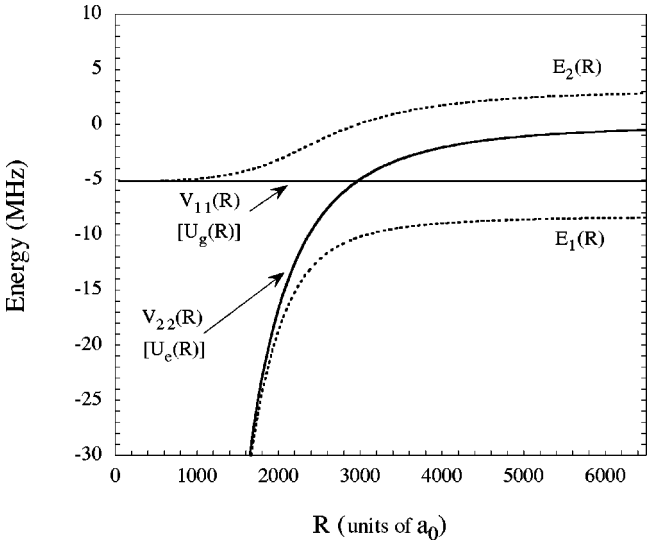

FIG. 2. The two-state model for trap loss collisions. The solid lines describe the bare (diabatic) quasimolecule potentials near the Condon point R_C. Here $\Delta=\gamma$, so $R_C\simeq 2930a_0$. The dotted lines describe the field-dressed (adiabatic) potentials.

sity matrix. The equation of motion for it, within the validity range of the WKB approximation, is

$$\frac{1}{2\mu}[p_i(r)+p_j(r)]\frac{d}{dr}\sigma_{ij}(r) = \sum_{kl}\left[\frac{p_i(r)p_j(r)}{p_k(r)p_l(r)}\right]^{1/2}[L_{ijkl}+\Gamma_{ijkl}]\sigma_{kl}(r), \tag{16}$$

where

$$L_{ijkl}=\frac{1}{i\hbar}[V_{ik}(r)\delta_{jl}-\delta_{ik}V_{lj}(r)]. \tag{17}$$

This completes the general derivation of the semiclassical optical Bloch equations using the Wigner distribution. The set of equations (16) was obtained by making a semiclassical approximation, which focuses on classical paths by virtue of using the WKB approximation. Only when the semiclassical approximation is valid (when the de Broglie wavelength is smaller than the region where the potentials are varying) will this approximation be meaningful.

The above derivation was done in the diabatic representation of the quasimolecule potentials. The decay term Γ has a simple form in this representation, where the electronic states are also independent of position, and the internal states are directly coupled by the standard dipole term. In the adiabatic representation the electronic wave functions vary with the internuclear coordinate R. In this presentation the laser-induced couplings and the decay term become clearly R dependent. We can move from the simple diabatic representation into the adiabatic one, in which the potential matrix V (which contains the radiative coupling) is diagonal. The transformation matrix $C(R)$ is R dependent,

$$\sum_{kl} C_{ik}^{-1}(R)V_{kl}(R)C_{lj}(R)=\delta_{ij}E_i(R), \tag{18}$$

where $E(R)$ is the diagonal eigenvalue matrix that gives the field-dressed quasimolecule potentials. We can now write the diabatic semiclassical density matrix in terms of the adiabatic semiclassical density matrix $\rho^a_{lk}(R,R';t)$:

$$\rho_{ij}(R,R';t)=\sum_{kl} C_{ik}(R)\rho^a_{kl}(R,R';t)C^{-1}_{lj}(R'). \tag{19}$$

Next we insert this $\rho_{lk}(R,R',t)$ into Eq. (3), and proceed as in the diabatic case. When making the WKB approximation and using the stationary phase approach we assume that the matrix elements $C_{ij}(R)$ are slowly varying functions in position. Thus, by sandwiching the whole equation between C^{-1} and C we obtain eventually

$$\frac{1}{2\mu}[p^a_i(r)+p^a_j(r)]\frac{d}{dr}\sigma^a_{ij}(r) = \frac{i}{\hbar}[E_j(r)-E_i(r)]\sigma^a_{ij}-\sum_{kl}\left\{Q_{ijkl}\frac{1}{2\mu}[p^a_k(r)+p^a_l(r)]-\Gamma^a_{ijkl}\right\}\sigma^a_{kl}(r)\left[\frac{p^a_i(r)p^a_j(r)}{p^a_k(r)p^a_l(r)}\right]^{1/2}, \tag{20}$$

where the classical momenta $p^a_i(r)$ are now defined using the adiabatic potentials $E_i(r)$ in Eq. (11). The decay term transforms as

$$\Gamma^a_{ijrt}=\sum_{klmn} C^{-1}_{ik}C_{lj}\Gamma_{klmn}C_{mr}C^{-1}_{tn}. \tag{21}$$

The nonadiabatic coupling that arose when we evaluated $\partial/\partial r[C\tilde{\rho}^a(r,t)C^{-1}]$ is given by

$$\begin{aligned}Q_{ijkl}&=\sum_m\left[C^{-1}_{im}(r)\frac{\partial}{\partial r}C_{mk}(r)\delta_{jl}+\delta_{ik}\frac{\partial}{\partial r}C^{-1}_{jm}(r)C_{ml}(r)\right]\\&=\sum_m\left[C^{-1}_{im}(r)\frac{\partial}{\partial r}C_{mk}(r)\delta_{jl}-\delta_{ik}C^{-1}_{jm}(r)\frac{\partial}{\partial r}C_{ml}(r)\right]\\&=A_{ik}(r)\delta_{jl}-\delta_{ik}A_{lj}(r),\end{aligned} \tag{22}$$

where $A_{ik}(r)=\Sigma_m C^{-1}_{im}(r)(\partial/\partial r)C_{mk}(r)$.

Another method for deriving the adiabatic OBE equations of motion involves using the half-collision matrix method [21]. This method yields the same result as given by Eqs. (20) and (22) for the Hamiltonian part of the dynamics, but cannot be used to derive the decay part of the adiabatic OBE equations, since the half-collision method does not incorporate the dissipative dynamics due to spontaneous emission contained in the density matrix treatment.

B. The two-state case

We assume that our quasimolecule has only two states, one ground state (1) and one excited state (2), with potentials V_{11} and V_{22}. In our trap loss model these states are as shown in Fig. 2. The excited state has a constant width γ, and the off-diagonal density matrix elements (ρ_{12} and ρ_{21}) have the width $\frac{1}{2}\gamma$. Thus we have

$$\Gamma_{1122}=\gamma, \quad \Gamma_{2222}=-\gamma, \quad \Gamma_{2121}=-\frac{1}{2}\gamma, \quad \Gamma_{1212}=-\frac{1}{2}\gamma, \tag{23}$$

and the rest of the elements of Γ are zero. Using V_{12} as the coupling between the states, we get the diabatic equations

$$\frac{d\sigma_{11}}{dr}=\frac{i}{\hbar}\frac{V_{12}}{\sqrt{v_1 v_2}}(\sigma_{12}-\sigma_{21})+\gamma\frac{\sigma_{22}}{v_2}, \tag{24}$$

$$\frac{d\sigma_{22}}{dr}=-\frac{d\sigma_{11}}{dr}, \tag{25}$$

$$\frac{d\sigma_{12}}{dr}=\frac{i}{\hbar}\frac{2(V_{11}-V_{22})+i\gamma}{v_1+v_2}\sigma_{12}-\frac{i}{\hbar}\frac{2V_{12}}{v_1+v_2}\times\left(\sqrt{\frac{v_1}{v_2}}\sigma_{22}-\sqrt{\frac{v_2}{v_1}}\sigma_{11}\right), \tag{26}$$

$$\frac{d\sigma_{21}}{dr}=\frac{d\sigma_{12}^*}{dr}. \tag{27}$$

Here we have used the classical velocities $v_i(r)=p_i(r)/\mu$.

In order to move into the adiabatic frame we need the transformation matrix elements, $C_{ij}(r)$. In a two-state system it is convenient to define

$$\theta=\frac{1}{2}\tan^{-1}\frac{2V_{12}}{V_{22}-V_{11}}. \tag{28}$$

The transformation matrix is given by

$$C(r)=\begin{pmatrix} C_{11} & C_{12} \\ C_{21} & C_{22}\end{pmatrix}=\begin{pmatrix} \cos(\theta) & \sin(\theta) \\ -\sin(\theta) & \cos(\theta)\end{pmatrix}, \tag{29}$$

and the inverse transformation is obtained from the relation $C^{-1}(\theta)=C(-\theta)$. Thus we get

$$A=C^{-1}\frac{\partial C}{\partial r}=\frac{\partial\theta}{\partial r}C^{-1}\frac{\partial C}{\partial\theta}=\frac{\partial\theta}{\partial r}\begin{pmatrix} 0 & 1 \\ -1 & 0\end{pmatrix}. \tag{30}$$

For convenience, we define $D=\partial\theta/\partial r$. This gives us

$$Q_{1121}=Q_{1222}=A_{12}=D, \quad Q_{1112}=-A_{21}=D,$$
$$Q_{1211}=-A_{12}=-D. \tag{31}$$

After a little algebra, we get the semiclassical optical Bloch equations in the adiabatic representation:

$$\frac{d\sigma_{11}^a}{dr}=-D\frac{v_1^a+v_2^a}{2\sqrt{v_1^a v_2^a}}(\sigma_{21}^a+\sigma_{12}^a)-\gamma\left[\frac{s^4}{v_1^a}\sigma_{11}^a-\frac{c^4}{v_2^a}\sigma_{22}^a+\frac{sc(c^2-s^2)}{2\sqrt{v_1^a v_2^a}}(\sigma_{21}^a+\sigma_{12}^a)\right], \tag{32}$$

$$\frac{d\sigma_{22}^a}{dr}=-\frac{d\sigma_{11}^a}{dr}, \tag{33}$$

$$\frac{d\sigma_{12}^a}{dr}=-\frac{2i}{\hbar}\frac{E_1-E_2}{v_1^a+v_2^a}\sigma_{12}^a-D\frac{2\sqrt{v_1^a v_2^a}}{v_1^a+v_2^a}(\sigma_{22}^a-\sigma_{11}^a)-\frac{\gamma}{v_1^a+v_2^a}\left\{\sigma_{12}^a+2s^2c^2(\sigma_{21}^a+\sigma_{12}^a)-\left[sc(1+2c^2)\sqrt{\frac{v_1^a}{v_2^a}}\sigma_{22}^a+sc(1+2s^2)\sqrt{\frac{v_2^a}{v_1^a}}\sigma_{11}^a\right]\right\}, \tag{34}$$

$$\frac{d\sigma_{21}^a}{dr}=\frac{d\sigma_{12}^a*}{dr}. \tag{35}$$

Here we use the notation $s=\sin(\theta)$ and $c=\cos(\theta)$. The velocity factors v_1^a and v_2^a are defined as in Eq. (11), using E_1 and E_2 as the appropriate potentials. At this point we relabel r with R.

C. The implementation of the two-state case

The optical Bloch equations (24)–(27) and (32)–(35) can be solved numerically using various methods. As will be shown in Sec. VII, the diabatic formulation fails when $T<1$ mK for all coupling strengths Ω. If we use the adiabatic equations (32)–(35), with the velocity factors given by Eq. (11), we find a good agreement with the MCWP results for all temperatures at large couplings, but an increasing deviation with decreasing Ω. Of course, we would like to have an approach that is good for all T and Ω. Thus we need to look into the issue of velocity factors in detail.

The velocity factor v_2^a for the upper adiabatic potential (see Fig. 2) is the source of the problem for small values of Ω. When the atoms approach each other, a steady state is quickly formed and maintained until the system gets very close to R_C. As discussed earlier, this gives us the advantage of a basis-independent initial state. At this point the population on the upper adiabatic state 2 is a steady state reflection of the population of the lower adiabatic state 1. Thus when the system reaches the Condon point the probability flux on both adiabatic states ought to in fact have the same momentum. Thus, if we use the velocity factor given by Eq. (11) for the upper adiabatic state, we get the right velocity asymptotically, but the wrong velocity at the crossing. We can correct this by redefining $v_2^a(R)$ so that $v_2^a=\sqrt{2E/\mu}$ for all R.

In other words, because the OBE approach mixes concepts from time-dependent theory (steady-state formation) and time-independent theory (WKB wave functions), we must sometimes improve its performance by such a tuning. Here we need to give the WKB wave functions asymptotically the velocities that describe the steady-state situation correctly, but at the crossing the dynamics dominates, implying that the classical momenta used in the time-independent theory would provide a more accurate description. Deviations are visible in the limit of the weak excitation, because then the excited state population is dominated by the small steady-state contribution that, due to the large momentum given incorrectly by Eq. (11), has a good chance to survive

on the excited state until $R=R_{\rm in}$. This population overwhelms the contribution from the dynamical excitation, and thus gives incorrect results. However, as will be shown in Sec. VII, we now have a method that can predict correctly the probability to reach small R on channel e for any practical Ω, and for the temperatures in the cold collisions regime. It should be noted that an extension of our approach to an ultracold temperature regime, i.e., below the recoil limit, is not likely to succeed, as the semiclassical viewpoint fails in this regime [22,23].

The previous formulation of optical Bloch equations [14] was done in the time frame rather than in the position frame. The transition between these two frames was performed by introducing a reference trajectory $v_0(R)$, which mapped R to t. However, as noted in Ref. [14], this reference trajectory is not really needed as we can do the calculation in the R frame altogether.

In practice when solving the optical Bloch equations we can set all $\sigma_{ij}(R_0)=0$, except selecting one state for which $\sigma_{ii}(R_0)=1$. The value of R_0 is set suitably large for the atoms to be well apart and potentials flat. Since the classical trajectory couples R and t, evolution in R corresponds to evolution in t and we find that the system has evolved into a steady state distribution of the ground- and excited-state populations after moving a relatively short distance towards smaller R. This corresponds to numerically determining the asymptotic state populations and coherences.

IV. MONTE CARLO SIMULATIONS

A direct wave-packet treatment of Eq. (1) with numerical methods is possible [6,7]. However, since one has to operate with a two-dimensional spatial grid, the memory sizes currently available in computers strongly limit the use of this approach: only models that are simplified in the extreme can be studied. In cold collisions the acceleration of the initially slow wave packet on the steep excited-state potential surface forces us to use a large two-dimensional momentum space while at the same time good momentum resolution is needed to define adequately the narrow initial wave packet for low temperatures. Similar demands are set for the position space as well; for more detailed discussion see Refs. [7,11]. Hence we need many grid points in order to span properly the required regions in both the momentum and position spaces.

It may be feasible to avoid some of the computational problems by using grid sizes and resolutions that are adaptive; one might utilize the rather deterministic behavior of the wave packet by altering the computational grid properties as a function of either position or time. Then the straightforward swapping between momentum and position representations using fast Fourier transforms is, however, usually lost. We have chosen to approach the problem from another angle. The Monte Carlo wave packet method allows us to treat Eq. (1) numerically as a one-dimensional problem. Unlike other approximative methods this approach does not adapt any concepts from classical mechanics and, therefore, it is not a semiclassical tool but a fully quantum one. Hence it can be used as a benchmark for the different semiclassical methods described in this article.

By using the MCWP method we can greatly diminish the limitations set by the available computer memory. However, this gain is partially reduced by the increase in the time required by the computation. Hence the MCWP simulations are quite time consuming, and therefore the need for other approaches is quite acute. There are several Monte Carlo approaches available currently, and we use the Dalibard-Castin-Mølmer version [24], adapted to wave packet problems in the manner described in Refs. [6,11,13]. We shall give here a brief description of the method, but keep the main emphasis on aspects related to the particular system studied in this article.

In the MCWP method one does not directly solve the time evolution of the density matrix itself. Instead, we look at the time evolution of the state vector

$$\Psi(R,t)=\begin{pmatrix}\Psi_g(R,t)\\ \Psi_e(R,t)\end{pmatrix}, \tag{36}$$

where Ψ_g and Ψ_e are the ground- and excited-state probability amplitudes, respectively. In this model the spontaneous decay appears as random quantum jumps during the time evolution of the state vector. Hence each time we solve the time-dependent Schrödinger equation we obtain a unique state vector evolution, also called a wave-packet history. One can form a finite ensemble of such histories and calculate ensemble averaged expectation values for physical quantities. These values are approximations to those provided by the full density matrix treatment. The accuracy of the ensemble averages tends to increase with the number of members in the ensemble, and in the limit of an infinite ensemble these averages and the density matrix results become equal, as shown, e.g., in Ref. [24]. So, we expect that by accumulating ensemble members we can eventually reach a suitable accuracy at some finite ensemble size. The accuracy to be expected of the method is described in Ref. [24]. For wave packets in cold collision problems the appropriate ensemble size seems to be roughly 50 members, assuming that all the histories are very close to each other in the phase space for all times. This is quite true for the excited-state survival studies related to attractive excited states. In general such localization in the phase space for all times is necessary for the success of the semiclassical approaches.

We start the calculation of the state vector evolution from some initial state, which in our case is a Gaussian wave packet on the ground state moving towards small R. The wave packet in general describes the probability to find the two colliding atoms at certain relative separation R, and its components $|\Psi_g(R,t)|^2$ and $|\Psi_e(R,t)|^2$ contain the additional information about how this probability is distributed between the ground and excited states. A Fourier transform of the state vector $\Psi(R,t)$ takes the system into the momentum representation. We set the initial phase of Ψ_g in position representation such that the wave packet starts with a mean momentum $\langle p\rangle$, which corresponds to the temperature of the cloud of cooled and trapped atoms. The width of the wave packet is chosen so that it remains relatively narrow in both representations. We cannot, of course, violate the Heisenberg uncertainty relation, so it is impossible to have infinitely narrow packets in either representation. It should be pointed out that apart from satisfying the Heisenberg uncertainty relation

the width of the wave packet is not related to any of the macroscopic quantities of the physical situation that we try to simulate.

Initially the wave packet is located far from the crossing so that a steady state between the ground and excited states can form before the wave packet reaches the interaction region where the dipole-dipole interaction makes the laser resonant with the molecular transition. The time scale for the formation of the steady state is roughly 3–5 times the decay time scale $1/\gamma_{\mathrm{mol}}$ [25], assuming that the local detuning does not change much over the distance covered by the wave packet during that time. As discussed above, the steady state formation allows us to put the initial wave packet on the diabatic ground state even when the laser-induced coupling is large asymptotically, because the final steady state is independent of the initial state. Indeed, we could even place the initial wave packet on the excited state, and yet the wave packet approaching the crossing would still be the steady-state one.

The state vector corresponding to the initial state is stepped forward in time with its evolution determined by the Schrödinger equation. Various numerical methods can be used, and we have applied the combination of split operator approach with Crank-Nicholson and Runge-Kutta algorithms, described in detail in Ref. [11]. In the MCWP method one uses an effective Hamiltonian,

$$H_{\mathrm{eff}}=H-i\frac{\hbar\gamma}{2}\sigma^{+}\sigma^{-}, \tag{37}$$

where H is the system Hamiltonian, γ is the decay rate for the excited-state population, and σ^{+} and σ^{-} are the standard spinor raising and lowering operators, respectively.

For each time step $t\rightarrow t+\delta t$ we calculate the jump probability

$$\delta s=\gamma P_e(t)\,\delta t, \tag{38}$$

where $P_e(t)$ is the current excited-state population. By rewriting δs as dP_e we would end up with the standard exponential decay $\exp(-\gamma t)$ of the excited-state population. Now, we continue by comparing the jump probability δs with a random number $\eta\in[0,1]$. A quantum jump occurs when $\eta<\delta s$; this is usually the less likely situation since the basic assumption in the derivation of the MCWP method is that $\delta s\ll 1$ all the time (guaranteed by choosing $\delta t\ll 1/\gamma$). When a jump occurs one simply replaces $\Psi_g(R,t+\delta t)$ with $\Psi_e(R,t+\delta t)$, and then sets $\Psi_e(R,t+\delta t)=0$. The occurrence of the jump corresponds to the observation of a fluorecence photon, which reduces the wave function: before the jump it had to be in the excited state, and after the jump it must be in the ground state. The important aspect is that as the jump takes place the position and momentum properties of the excited-state component of the state vector are transferred to the ground-state component. This is the source of radiative heating, among other things.

Both the evolution under H_{eff} and the quantum jumps reduce the norm of the state vector Ψ. Hence after each time step the state vector is renormalized to unity, even if a jump does not occur. It should be noted that if we had $H_{\mathrm{eff}}=H$, then we would always observe a quantum jump for a system with nonzero P_e if we wait long enough. For cases where $P_e<1$ this would be wrong, since there is a nonzero probability that the system never was on the excited state. In the weak field limit P_e is always very small, so most of the ensemble members correspond to the time evolution under the non-Hermitian Hamiltonian with no interruption by jumps. Then the wave packet approach reduces to a time-dependent version of the complex potential approach. Therefore a single ensemble member becomes a reasonably accurate approximation to the density matrix result. We have used this property in our weak field study [12], and have thus verified that the diabatic formulation of the OBE method does not work properly at low temperatures, but the Landau-Zener approach and the complex potential method can be used instead.

Although the MCWP method allows us to use relatively large grids, the strong change in the excited-state potential corresponds at our probing distance $R_{\mathrm{in}}=143a_0$ to kinetic energies that are beyond the numerical treatment. Basically it becomes impossible to correctly track the relevant quantum mechanical phase term $\exp(-iE\delta t/\hbar)$, where E is the kinetic energy of the wave packet. Hence we must cut the excited-state potential change by making it flat for $R_{\mathrm{in}}<R<R_{\mathrm{cut}}$; in our studies we have used the value $R_{\mathrm{cut}}=512a_0$. At R_{cut} we are basically left with the exponential decay of the excited-state population because of the large local detuning. Hence we can take the wave packet result for $J_e(R)$ from $R=R_{\mathrm{cut}}$ to R_{in} by multiplying it with $\exp(-\gamma t_{\mathrm{trans}})$, where t_{trans} is the time it takes to go from R_{cut} to R_{in} along the classical path determined by the local velocity. In fact, the same approach is also applied when the OBE equations are solved numerically: otherwise the adequate determination of the term $\exp[-ip(R)\delta R/\hbar]$ would require impractically small values of the spatial grid spacing δR [here $p(R)$ is the local momentum at R] when $R<R_{\mathrm{cut}}$.

V. COMPLEX POTENTIAL CALCULATIONS

In the complex potential method one adds a complex term on the excited-state potential in order to describe decay out of these states [10,15,16]. This approach does not allow any reexcitation, and is thus not appropriate for strong field studies directly (by including the photon states explicitly one might improve the model although this would drastically increase the number of channels required to solve even the case of two quasimolecule states [16]).

In this method one simply uses the Hamiltonian

$$H=T(R)+\begin{pmatrix} U_g(R)+U_c(R,l) & \hbar\Omega & 0 \\ \hbar\Omega & \hbar\Delta+U_e(R)+U_c(R,l)-i\hbar\gamma/2 & \hbar\Omega_{ep} \\ 0 & \hbar\Omega_{ep} & E_p+U_p(r)+U_c(R,l) \end{pmatrix}, \tag{39}$$

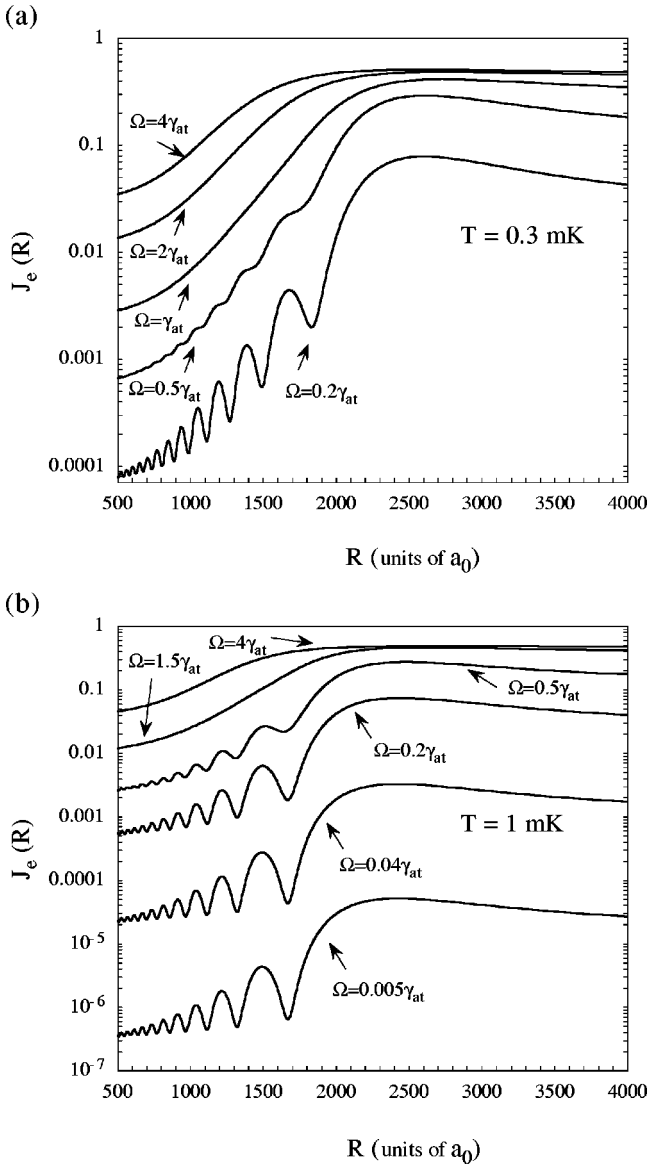

FIG. 3. The excited-state flux $J_e(R)$ calculated using the MCWP method. Here $\Delta=\gamma_{\rm at}$, and the other parameters are as indicated in the figure.

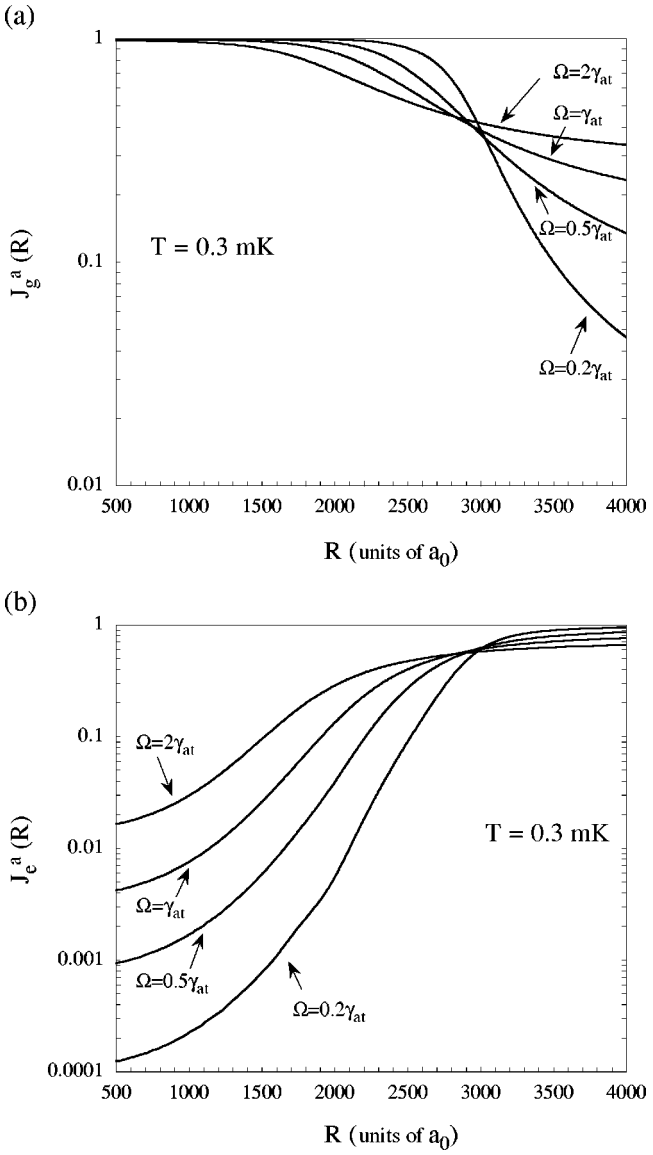

FIG. 4. The ground- and excited-state fluxes $J_g^a(R)$ (a) and $J_e^a(R)$ (b) in the adiabatic representation, calculated using the A-OBE method. Here $\Delta=\gamma_{\rm at}$, and the other parameters are as indicated in the figure.

and solves the time-independent Schrödinger equation

$$\frac{d^2F(R)}{dR^2}+\frac{2\mu}{\hbar^2}[E-U(R)]F(R)=0, \tag{40}$$

where F is the three-component state vector for our model and E is the asymptotic collision energy.

For this method we have explicitly included the probe channel p to our Hamiltonian: $U_p(R)$ is the corresponding potential. The probe channel p crosses the e channel potential at $R_{\rm in}$. Because of the disparity between $R_C(\Delta)$ and $R_{\rm in}$ the outer zone excitation process is in practice well separated from the inner zone process. The coupling Ω_{ep} depends on the nature of the coupling of the excited state and the probe channel.

We have used the invariant imbedding method [15,26] (in the diabatic representation) to solve the above close coupling equations in a form that directly computes the S matrix elements, S_{gp} and S_{ep}, from which the quantum flux $J_e(R)$, i.e., the quantum mechanical probability of reaching the inner zone, is determined. In the complex potential calculations we use mainly the same values for parameters as in the two-state model, given in Sec. II. However, here the excited-state potential, $U_e(R)$, is taken as a numerical spline having a minimum energy of -182 GHz at $R=72a_0$ and an asymptotic behavior of $-C_3/R^3$. We take the probe potential to be $U_p(R)=C_3^p/R^3$, with $C_3^p=7.260e^2a_0^2$. All potentials have repulsive inner walls so the $R<0$ region is nonclassical. The other parameters are $E_p=-3.0$ GHz and $\Omega_{ep}=1.0$ MHz.

As we are now working with the time-independent scattering theory, we need to consider boundary conditions instead of initial ones. Since the model potential contains nonvanishing off-diagonal elements, for strong fields there is a clear mixing of states at large R. Therefore the boundary condition for the complex potential approach has to be de-

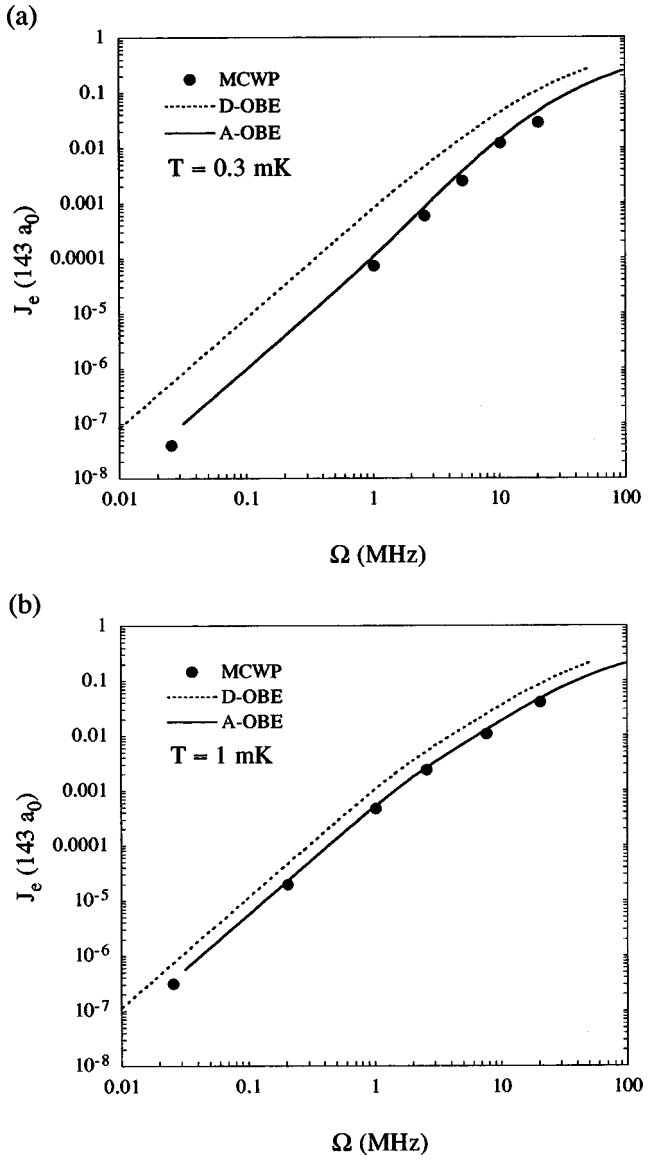

FIG. 5. The excited-state flux J_e at $R=143a_0$ as a function of the laser-induced coupling Ω, calculated using the MCWP, D-OBE, and A-OBE methods. Here $\Delta=\gamma_{\rm at}$, and the other parameters are as indicated in the figure.

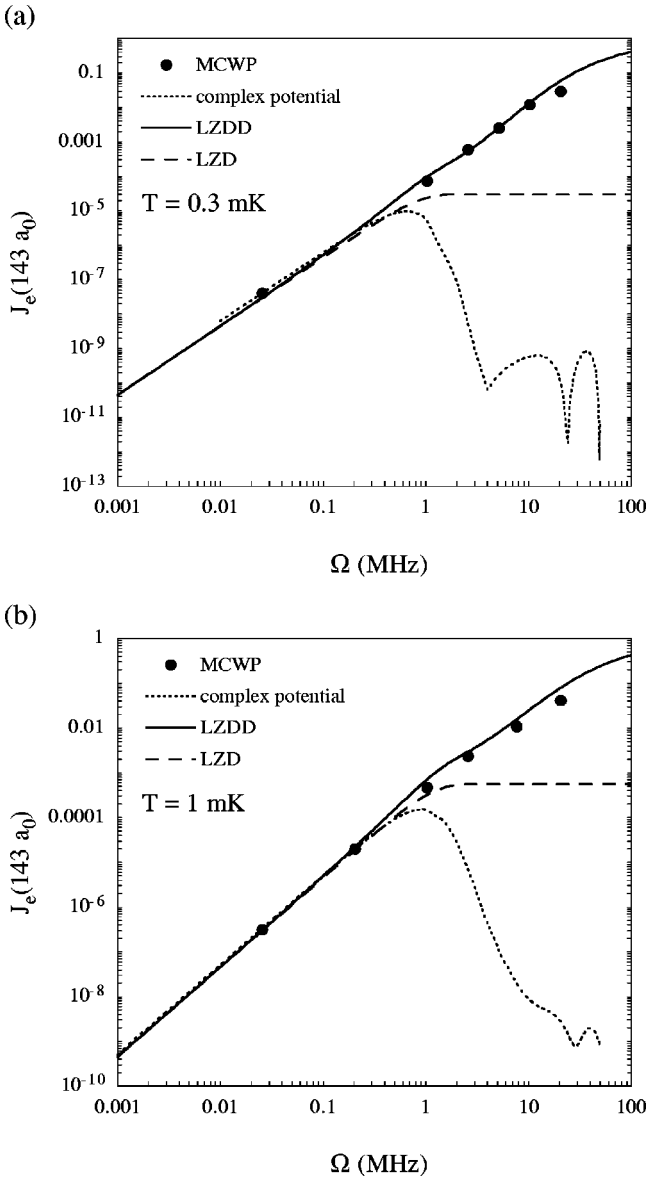

FIG. 6. The excited-state flux J_e at $R=143a_0$ as a function of the laser-induced coupling Ω, calculated using the MCWP, complex potential, LZD, and LZDD methods. Here $\Delta=\gamma_{\rm at}$, and the other parameters are as indicated in the figure.

fined in terms of the field-dressed, i.e., adiabatic states. The transformation between the different bases then takes place as described in Sec. III. We assume an incoming wave (corresponding to the asymptotic collision energy E) on the lower adiabatic channel formed by states g and e (state 1 in Fig. 2).

VI. LANDAU-ZENER APPROACHES

Since the inner and the outer crossings are isolated in distinctly different regions, we can write the loss probability, i.e., the probability to exit on channel p as

$$P_p=|S_{gp}|^2=P_{ep}(R_{\rm in})J_e(R_{\rm in}), \tag{41}$$

where the probability $P_{ep}=|S_{ep}|^2$ measures the quantum probability of the inner zone $e\rightarrow p$ process due to traversing the inner curve crossing once in both directions. Here $R_{\rm in}$ is the location of this curve crossing. When using the complex potential method we obtain the flux simply by using the relation $J_e(R_{\rm in})=|S_{gp}|^2/P_{ep}(R_{\rm in})$. The probability P_{ep} is almost completely insensitive to the laser intensity I and to the collision energy E for small detunings.

In the limit of large detuning and small laser intensity it is safe to assume that the excitation becomes localized to the Condon point R_C. In this limit the dynamical model and the local equilibrium model tend to agree. In local equilibrium models one assumes that the motion of the atoms is very slow compared to the steady-state formation, and thus the steady-state formation dominates [8]. This leads to a picture where off-resonant excitation is important for small Δ. One can express the local excitation in a two-state model in the steady state regime as [25]

$$\sigma_{ee}=\frac{\Omega^2}{\Delta(R)^2+2\Omega^2+(\gamma/2)^2}, \tag{42}$$

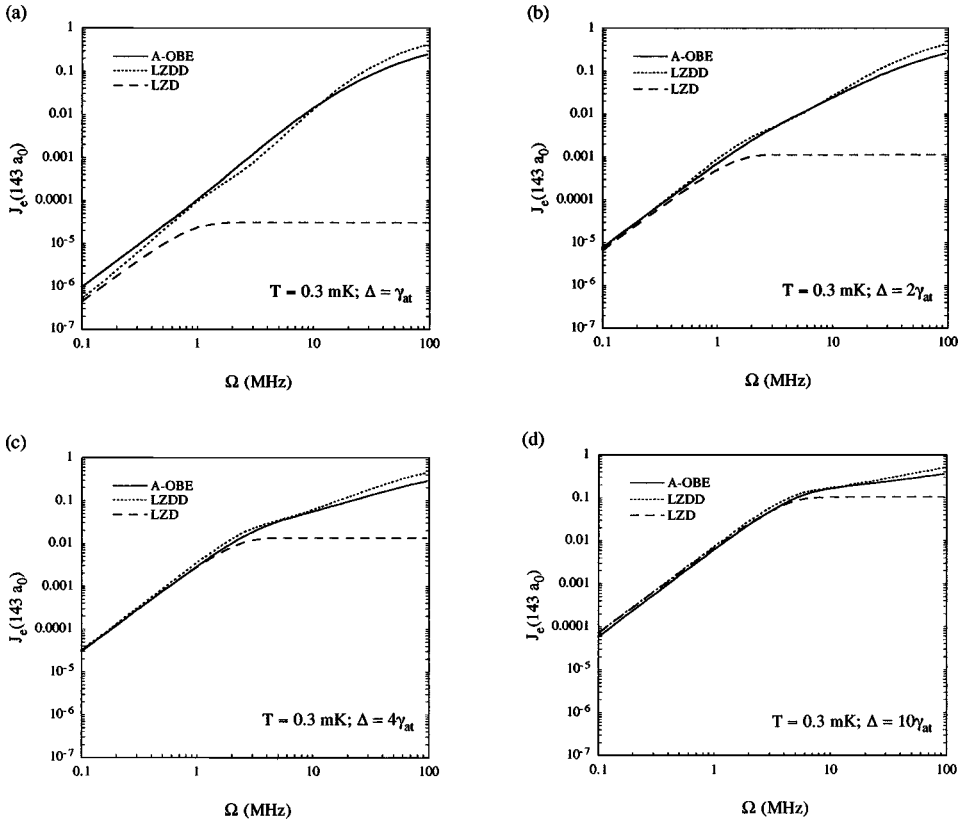

FIG. 7. The excited-state flux J_e at $R=143a_0$ as a function of the laser-induced coupling Ω, calculated using the A-OBE, LZD, and LZDD methods for $T=0.3$ mK.

where $\Delta(R)$ is the local detuning, $\hbar\Delta(R)=U_e(R)-U_g(R)+\hbar\Delta$. As a final stage in the local equilibrium model one weighs the results with Eq. (42) and integrates over the position coordinate R.

In the dynamical models it is assumed that as the system approaches R_C the motion and thus the change in the local detuning become fast compared to the steady-state formation, and thus the excitation becomes a dynamical process that is localized to a region near R_C. The dynamical excitation can then be described with the Landau-Zener curve crossing model [10–13]. In steady-state models for large detunings the integration over the linewidth function (42) becomes like a δ function that singles out the Condon point, and thus the two viewpoints agree in this limit. The MCWP simulations have so far supported the dynamical picture over the local equilibrium picture; for further discussion see Ref. [3].

In the weak field limit we can assume that the excitation and subsequent decay are uncoupled, and reexcitation is negligible. Then we can write, using the Landau-Zener model, the expression for the flux on channel e as

$$J_e^{\mathrm{LZD}}(R)=S_e(R,R_C;E,\gamma)P_{\mathrm{LZ}} =S_e(R,R_C;E,\gamma)[1-\exp(-2\pi\Lambda)]. \quad (43)$$

Here

$$\Lambda=\frac{\hbar\Omega^2}{\alpha v_g(R_C;E)}, \quad (44)$$

where $v_g(R;E)$ is the classical velocity associated with the ground state at position R when the collision energy is E, and

$$\alpha=\left|\frac{dU_e(R)}{dR}-\frac{dU_g(R)}{dR}\right|_{R=R_C}. \quad (45)$$

In other words, P_{LZ} is the one-way Landau-Zener probability of undergoing a transition from channel g to channel e at the Condon point $R_C(\Delta)$, and $S_e(R,R_C;E,\gamma)$ is the survival probability from R_C to R. We can calculate the survival probability by assuming a classical trajectory combined with exponential (Weisskopf-Wigner) decay:

$$S=\exp(-\gamma t_{\mathrm{cl}}); \quad t_{\mathrm{cl}}(R,R_C;E)=\int_{R_C}^{R}\frac{dR}{v_e(R)}, \quad (46)$$

where $v_e(R)$ is the classical trajectory velocity for the excited state (in the diabatic formulation). This is the Landau-Zener model with decay (LZD).

The above model fails when excitation and decay do not decouple, which happens at strong fields due to reexcitation of decayed population [11,13]. We can think of reexcitation as a process that delays the start of the exponential decay. Reexcitation takes place mainly within some region around the Condon point. We can define an interaction region for which $\Delta(R)<\Omega$. By making the simple assumption that exponential decay can take place only outside this region, we can rewrite the t_{cl} in Eq. (46) as

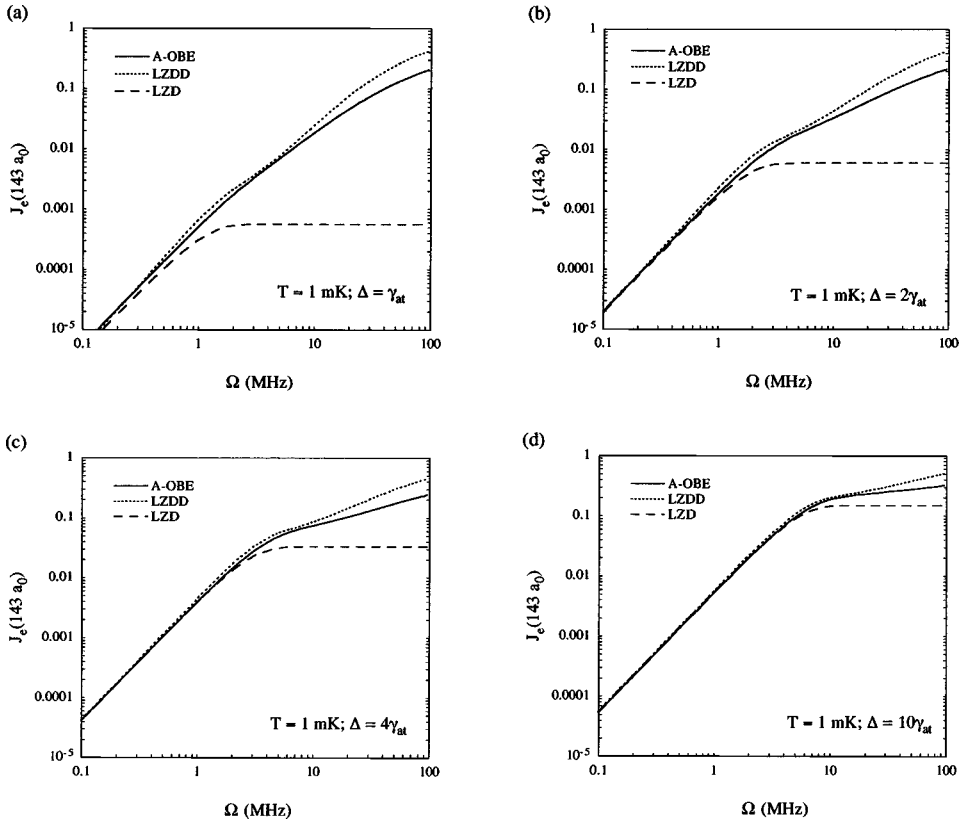

FIG. 8. The excited-state flux J_e at $R=143a_0$ as a function of the laser-induced coupling Ω, calculated using the A-OBE, LZD, and LZDD methods for $T=1.0$ mK.

$$t_{\mathrm{cl}}=\int_{R_\Omega}^{R}\frac{dR}{v_e(R)}, \tag{47}$$

where R_Ω is defined by the relation $\Delta(R_\Omega)=\Omega$; $R_\Omega<R_C$. The modified survival term depends now on the laser intensity I ($I\propto\Omega^2$). We call this approach the Landau-Zener model with delayed decay (LZDD). Obviously the model can only give qualitative predictions, especially as the concept of the edge of the interaction region is not well defined. However, it gives a good intuitive undestanding of why $J_e(R)$ for small R keeps increasing even when the excitation saturates to unity (and thus the LZD prediction saturates) [18]. This picture agrees qualitatively with the results from the OBE and MCWP calculations, as will be shown in the next section.

VII. COMPARISON OF METHODS

Typically the excited-state flux $J_e(R)$ shows oscillations at $R<R_C$ in the bare state picture. This is demonstrated by the MCWP results given in Fig. 3. The oscillations are due to the coherences between the two states, established near the Condon point. As the coupling Ω increases, the situation becomes increasingly adiabatic and the oscillations disappear. At the same time the asymptotic (large R) flux approaches the steady-state result, 1/2. It is interesting to note that although the main change in the flux seems to take place over a wide region in R, the dynamical view with excitation localized to R_C works well, as demonstrated by us earlier in Ref. [12].

We also have calculated the R dependence of the probability fluxes [$J_g^a(R)$ and $J_e^a(R)$] in the adiabatic presentation using the adiabatic OBE method; the results are shown in Fig. 4 for $T=0.3$ mK and selected values of Ω. For very small Ω the lower adiabatic state correlates asymptotically with the diabatic ground state. At small R it correlates with the excited diabatic state for all Ω. As expected, no oscillations are present in the adiabatic representation as a function of R.

In Fig. 5 we show a comparison between the MCWP results, the diabatic OBE results (D-OBE), and adiabatic OBE results (A-OBE). The agreement between the MCWP and A-OBE results is very satisfactory, whereas the D-OBE results fail by an order of magnitude for $T=0.3$ mK. This failure increases further as T decreases, as shown in Refs. [10,12]. As discussed in the previous paragraph, the difference between D-OBE and A-OBE results suggest strongly that the basic condition for the validity of the local equilibrium model is not fulfilled for typical trap parameters.

We compare the complex potential method and the Landau-Zener approaches to the MCWP results in Fig. 6. The LZD method saturates when the Landau-Zener excitation probability P_{LZ} becomes unity; until then all methods seem to agree well. However, beyond the saturation of the excitation the complex potential approach fails utterly. One should note that the saturation of the dynamical excitation is not the same as the saturation of the atomic excitation (also, the atomic excitation saturates to 1/2, but the dynamical excitation to unity). The complex potential method fails utterly when one approaches the saturation limit. The LZDD

method agrees well with the MCWP results.

We have used the A-OBE and LZDD method to calculate the flux for various detunings, and the results are given in Figs. 7 and 8. As can be expected, the saturation moves to larger Ω when Δ increases. In Fig. 7(a) we start to see the signs of the failure of the Landau-Zener model at small T (and small Δ).

VIII. CONCLUSIONS

In this paper we have derived the adiabatic optical Bloch equations. When applied to the standard two-state model for loss of laser-cooled atoms from electromagnetic traps, these equations prove to be a fast and adequately accurate method to predict probabilities to reach any internuclear distance on the excited quasimolecule state. The A-OBE results match very well with the MCWP results, and also agree with the results from the qualitative LZDD model. The latter agreement is surprisingly good, but this can be attributed to a fortuitous definition of the edge of the interaction region.

Although the A-OBE method is a useful tool, we are still far from having a proper general treatment of trap loss at small detunings. Firstly, the bound state structure of the attractive excited state is not taken into account. At small detunings the vibrational states associated with the attractive molecular potential overlap strongly and at strong fields they are also power broadened. In the language of time-dependent approach, the first ''vibration'' of the quasimolecule dominates over all the others. We can remedy the situation to some extent by applying the single passage result to multiple passages, as has been done, e.g., in Ref. [27].

Secondly, the A-OBE method does not allow for momentum change; the motion on the ground state is given by the ground-state velocity factor. When the excited-state population of the quasimolecule decays back to the ground state, its kinetic energy distribution has been affected by the acceleration on the excited state. If this population is excited by, e.g., another laser, this excitation depends on the new kinetic energy distribution. This effect is important in the cases of radiative heating [11] and the radiative enhancement [28,29]. Currently only the MCWP method can handle the kinetic energy changes correctly [11].

Thirdly, the velocity factors diverge at classical turning points. Thus the A-OBE method is not capable of treating the case of optical shielding [3,13], which involves excitation to a repulsive quasimolecule potential by a blue-detuned laser. This problem might be solved by replacing the WKB wave function by a proper Airy function solution in our derivation of the A-OBE method [30].

Finally, we have given here as an example only the case of one ground state and one excited state. In reality we have several states involved in the cold collision process, e.g., the various partial waves and hyperfine states. In such a situation it is not so easy to write out the transformation to the adiabatic representation in an analytic form. However, there are various methods for doing the change of basis numerically. A problem may arise from the fact that we had to redefine the velocity factors using physical arguments—it is not obvious if such a redefinition in a multistate case would be as straightforward and clear as in the two-state case. In any case, the A-OBE method should be capable of handling adequately the case of several partly overlapping strong crossings in a system of close-lying states. In such a situation the Landau-Zener methods are expected to fail—the A-OBE method can help in testing the validity of the Landau-Zener methods in nontrivial crossing situations.

For small detunings the Condon point moves to very large distances and the quasimolecule potential does not have the simple $1/R^3$ dependence any more. Furthermore, the retardation effects become important, and then the quasimolecular linewidths become R dependent even in the diabatic representation. The A-OBE method should be very useful in studying these situations, as it is much faster than the MCWP method when exploring a wide range of cases with varying laser parameters (Δ and Ω) and quasimolecule potentials (C_3, l).

Despite some limitations the A-OBE method is a clear leap forward in treating theoretically the cold collisions in light fields. The discussion above, however, should be taken as a warning against trusting the method too blindly. The results given in this paper and in our previous report [18] indicate nevertheless that the method is very good in predicting the behavior of trap loss due to near-resonant light.

ACKNOWLEDGMENTS

This work was supported in part by grants from the U.S.–Israel Binational Science Foundation and the Office of Naval Research. K.B. and K.-A.S. thank the U.K. EPSRC for financial support. K.-A.S. thanks the Academy of Finland for financial support. The authors also thank Fred Mies for useful comments.

[1] P. D. Lett, P. S. Julienne, and W. D. Phillips, Annu. Rev. Phys. Chem. **46**, 423 (1995).

[2] P. S. Julienne, A. M. Smith, and K. Burnett, Adv. At., Mol., Opt. Phys. **30**, 141 (1993).

[3] K.-A. Suominen, J. Phys. B **29**, 5981 (1996).

[4] T. Walker and P. Feng, Adv. At., Mol., Opt. Phys. **34**, 125 (1994); J. Weiner, Adv. At., Mol., Opt. Phys. **35**, 45 (1995).

[5] J. von Neumann, *Mathematical Foundations of Quantum Mechanics* (Princeton University Press, Princeton, 1955); L. van Hove, Physica (Amsterdam) **21**, 517 (1955); E. B. Davis, *Quantum Theory of Open Systems* (Academic Press, London, 1976); L. Allen and J. H. Eberly, *Optical Resonance and Two Level Atoms* (Dover, New York, 1987); R. Alicki and K. Lendi, *Quantum Dynamical Semigroups and Applications* (Springer, New York, 1987); H. Carmichael, *An Open Systems Approach to Quantum Optics* (Springer, Berlin, 1993); S. Stenholm and M. Wilkens, Contemp. Phys. **38**, 257 (1997).

[6] W. K. Lai, K.-A. Suominen, B. M. Garraway, and S. Stenholm, Phys. Rev. A **47**, 4779 (1993).

[7] K.-A. Suominen and B. M. Garraway, Phys. Rev. A **48**, 3811 (1993).

[8] A. Gallagher and D. E. Pritchard, Phys. Rev. Lett. **63**, 957 (1989).

[9] P. S. Julienne and J. Vigué, Phys. Rev. A **44**, 4464 (1991).

[10] P. S. Julienne, K.-A. Suominen, and Y. B. Band, Phys. Rev. A **49**, 3890 (1994).
[11] M. J. Holland, K.-A. Suominen, and K. Burnett, Phys. Rev. Lett. **72**, 2367 (1994); Phys. Rev. A **50**, 1513 (1994).
[12] K.-A. Suominen, M. J. Holland, K. Burnett, and P. S. Julienne, Phys. Rev. A **49**, 3897 (1994).
[13] K.-A. Suominen, M. J. Holland, K. Burnett, and P. S. Julienne, Phys. Rev. A **51**, 1446 (1995).
[14] Y. B. Band and P. S. Julienne, Phys. Rev. A **46**, 330 (1992).
[15] I. Tuvi and Y. B. Band, J. Chem. Phys. **99**, 9697 (1993).
[16] H. M. J. M. Boesten, B. J. Verhaar, and E. Tiesinga, Phys. Rev. A **48**, 1428 (1993); H. M. J. M. Boesten and B. J. Verhaar, *ibid.* **49**, 4240 (1994).
[17] R. Napolitano, J. Weiner, C. J. Williams, and P. S. Julienne, Phys. Rev. Lett. **73**, 1352 (1994).
[18] Y. B. Band, I. Tuvi, K.-A. Suominen, K. Burnett, and P. S. Julienne, Phys. Rev. A **50**, R2826 (1994).
[19] A. Fioretti, J. H. Müller, P. Verkerk, M. Allegrini, E. Arimondo, and P. S. Julienne, Phys. Rev. A **55**, R3999 (1997).
[20] M. Hillery, R. F. O'Connell, M. O. Scully, and E. P. Wigner, Phys. Rep. **106**, 121 (1984).
[21] F. H. Mies and P. S. Julienne, J. Chem. Phys. **80**, 2526 (1984); Y. B. Band and F. H. Mies, *ibid.* **88**, 2309 (1988); R. L. Dubs, P. S. Julienne, and F. H. Mies, *ibid.* **93**, 8784 (1990).
[22] K. Burnett, P. S. Julienne, and K.-A. Suominen, Phys. Rev. Lett. **77**, 1416 (1996).
[23] P. S. Julienne, NIST J. Res. **101**, 487 (1996).
[24] J. Dalibard, Y. Castin, and K. Mølmer, Phys. Rev. Lett. **68**, 580 (1992); Y. Castin, K. Mølmer, and J. Dalibard, J. Opt. Soc. Am. B **10**, 524 (1993).
[25] R. Loudon, *The Quantum Theory of Light*, 2nd ed. (Oxford University Press, Oxford, 1983).
[26] S. J. Singer, K. F. Freed, and Y. B. Band, J. Chem. Phys. **77**, 1942 (1982).
[27] M. G. Peters, D. Hoffmann, J. D. Tobiason, and T. Walker, Phys. Rev. A **50**, R906 (1994).
[28] K.-A. Suominen, K. Burnett, P. S. Julienne, M. Walhout, U. Sterr, C. Orzel, M. Hoogerland, and S. L. Rolston, Phys. Rev. A **53**, 1678 (1996).
[29] V. Sanchez-Villicana, S. D. Gensemer, and P. L. Gould, Phys. Rev. A **54**, R3730 (1996).
[30] M. S. Child, *Semiclassical Mechanics with Molecular Applications* (Oxford University Press, Oxford, 1991).